Kidney International, Vol. 57 (2000), 2546–2556

DIALYSIS – TRANSPLANTATION

Computer simulations of ultrafiltration profiles for an icodextrin-based peritoneal fluid in CAPD

BENGT RIPPE and LARS LEVIN

Department of Nephrology, University Hospital of Lund, Lund, Sweden

Computer simulations of ultrafiltration profiles for an icodextrin-based peritoneal fluid in CAPD.

Background. The three-pore model of peritoneal transport has the ability to predict ultrafiltration (UF) profiles rather accurately, even when high molecular weight (MW) solutes are employed as osmotic agents in continuous ambulatory peritoneal dialysis (CAPD). In the present simulations, we wanted to assess, for various theoretical perturbations, the UF properties of a peritoneal dialysis (PD) solution with an osmotic agent having an average MW of 20 kD and a "number average MW" of 6.2 kD, which is similar to that of icodextrin (ICO).

Methods. For a PD solution containing a completely monodispersed 20 kD MW osmotic agent, the degree of UF modeled is much higher than that reported for ICO. Hence, to model the behavior of ICO, we subdivided the ICO molecules into eight or more different MW size fractions. For simulations using six or eight subfractions, we obtained an excellent fit of simulated to reported UF data. More dispersed solutions produced UF profiles similar to that with eight fractions.

Results. A 2.05 L 7.5% ICO PD solution, despite being slightly hypotonic, yielded a UF volume of nearly 600 mL in 12 hours, modeled for patients not previously exposed for ICO. After nine hours, the UF volume exceeded that produced by 3.86% glucose. The UF rate and volumes increased in proportion to (*1*) the ICO concentration, (*2*) the peritoneal surface area, and (*3*) the peritoneal UF coefficient, but was almost insensitive to increases in the instilled fluid volume. Simulated for patients previously exposed to ICO, having steady-state plasma concentrations of ICO degradation products, the predicted UF volume at 12 hours was reduced to approximately 400 mL.

Conclusion. Employing the three-pore model of peritoneal transport and taking into account the polydispersed nature of ICO, it was possible to accurately computer simulate the UF profiles of ICO in accordance with reported data. The simulations suggest an advantage of using ICO in patients with type I UF failure, where UF with a high-MW osmotic agent will exceed that seen in patients not showing UF failure who are on glucose-based PD solutions.

Key words: dialysate, membrane permeability, three-pore model of peritoneal transport, fluid and solute transport.

Received for publication August 19, 1999
and in revised form December 14, 1999
Accepted for publication December 17, 1999

The three-pore model of peritoneal transport has been successfully employed to predict ultrafiltration (UF) profiles in continuous ambulatory peritoneal dialysis (CAPD) in normal and a number of perturbed conditions [1, 2]. The model assumes the presence of a large number of small pores (radius 40 to 50 Å) in the peritoneal membrane, permeable to most small solutes and water, together with a very low number of large pores (radius ≈250 Å), allowing the transport of macromolecules from blood to peritoneum. A third transperitoneal exchange route is predicted to conduct water via "ultrasmall pores" in the plasmalemma of radius ≈3 to 5 Å, which rejects solute transport, denoted aquaporins [3, 4]. Aquaporins play an important role in peritoneal osmotic water transport and in solute sieving. They seem to provide an explanation for the apparent paradox that the rather "open" peritoneal membrane actually effectively "sieves" small solutes from water when UF is driven by high crystalloid (glucose) osmotic gradients [2].

Compared with traditional models, such as that described by Pyle, Moncrief, and Popovich (P&P) [5] and Vonesh et al [6], small solute reflection coefficients are approximately one order of magnitude lower and the peritoneal UF coefficient approximately tenfold higher in the three-pore model. According to the P&P model, for example, there is hardly any difference in osmotic efficiency among solutes of different sizes. However, the three-pore model seems to yield realistic estimates of small-solute reflection coefficients, which are less than 0.1, while those of larger solutes approach unity. The three-pore model thus explains why high molecular weight (MW) solutes are more efficient on a molar basis as osmotic agents in PD than small solutes [7], and it has been demonstrated to be superior to previous models in predicting UF profiles for high-MW osmotic agents [8].

The present study deals with the rather complex computer modeling of a macromolecular osmotic agent, namely, glucose polymers or dextrins, using the three-pore model of peritoneal transport [2, 9]. Icodextrin (ICO) is a polydispersed glucose polymer having a MW distribution such that 85% of the molecules have a MW

between 1638 and 45000 D, and 6% less than 1638 D. The weight average MW is around 16 to 20 kD, and the number average MW is less than 6.5 kD [10–13]. Actually, a majority of the molecules in the ICO preparation have a MW of less than 3 kD. Although ICO is very polydispersed, previous attempts to theoretically analyze the clinical UF profiles for ICO have not taken its polydispersity into account [14]. In the present simulations, however, polydispersity was accounted for by subdividing the ICO molecules into eight major size fractions, which yielded UF profiles compatible with data in the literature. The aim of the present study was to simulate a number of different physiological and pathophysiological scenarios compatible with different clinical situations encountered in peritoneal dialysis, and to predict the UF profiles for ICO in these situations.

METHODS

Parameter selection

The three-pore model has been described at some length elsewhere [1, 2, 8, 9, 15]. Basically, the three-pore model conceives the capillary membrane (the endothelium) as the limiting barrier for solute and fluid transport between blood and dialysate, more or less neglecting the interstitium and any concentration gradients herein. In this work, the three-pore model was slightly modified from its original version by setting the small pore radius at 43 Å, the UF coefficient at 0.074 mL/min/mm Hg, and the fraction of the UF coefficient accounted for by the aquaporins at 0.02. All of these values were obtained from parameter optimization procedures based mainly on data from previous studies on glucose-based dialysis fluids [15, 16]. Dextrin's molecular radii (a_e) was obtained from $a_e = 0.486\ (MW)^{0.385}$ [1], and dextrin permeability-surface area products [PS or mass transfer area coefficients (MTACs)] were assessed from the theory of restricted diffusion (and convection) across membranes having cylindrical pores (pore theory), setting the "area parameter" ($A_0/\Delta X$) at 25,000 (cm) [2, 16]. Dextrin clearance out of the peritoneal cavity was set at (PS + 1.2) mL/min to account for the transcapillary clearance (PS) and the clearance to peritoneal tissues (~1.2 mL/min). Direct lymphatic clearance (0.3 mL/min) was added separately [1]. The simulations were performed assuming that the patients had not been previously exposed to ICO, except in one case, in which we also tried to model a situation relevant to that during long-term use of ICO. The parameters used for the computer simulations are shown in Table 1. The major equations employed and the calculation techniques applied are found in the **Appendix**. A fourth- to fifth-order Runge-Kutta algorithm (Maple V software) was employed to carry out the integrations of the differential equations, describing the osmotic flow across each of the three subsets of membrane pores in order to produce the simulated UF profiles.

Table 1. Parameters used for computer simulations of intraperitoneal volume versus time [V(t)] curves according to a three-pore model of membrane selectivity

Small pore radius (r_s) *Å*	43
Large pore radius (r_L) *Å*	250
Fractional small pore UF coefficient (α_s)	0.900
Fractional transcellular UF coefficient (α_c)	0.020
Fractional large pore UF coefficient (α_L)	0.080
Ultrafiltration coefficient (L_pS) *mL/min/mm Hg*	0.074
Osmotic conductance to glucose ($L_pS\ \sigma_g$) *μL/min/mm Hg*	3.6
"Unrestricted" pore area over unit diffusion distance for small pores $(A_0/\Delta X)_s$ cm	25,000
PS ("MTAC") for glucose *mL/min*	15.4
PS ("MTAC") for "Na" and "an" *mL/min*	6.0
Peritoneal lymph flow (L) *mL/min*	0.3
Transperitoneal hydrostatic pressure gradient (ΔP) *mm Hg*	8
Transperitoneal oncotic pressure gradient ($\Delta\pi_{prot}$) *mm Hg*	22
Dialysis fluid volume instilled *mL*	2050
Peritoneal residual volume (V_r) *mL*	300
Serum urea concentration *mmol/L*	20
Serum sodium (and sodium associated "anion" concentration) *mmol/L*	140
Serum glucose concentration *mmol/L*	6.5
Dissociation factor for "Na" and "an"	0.93

Mass and osmolality spectrum of ICO

Icodextrin is a polydispersed preparation, with 5 to 6% of the mass spectrum in the 0.18 to 1.6 kD MW range and 8 to 9% of the mass spectrum above 45 kD in MW [10]. Approximately 80% of the mass, however, is represented by molecules having MWs ranging from 10 to 30 kD. An attempt to mimic this spectrum, a procedure using eight subfractions of ICO, was used in this study. This is shown in Figure 1A, where the percentage of total osmolality or total preparation weight in each of the fractions is plotted versus log MW. This spectrum should be rather close to that used in commercial preparations of ICO [10–12]. Note that the osmolality spectrum, which determines the osmotic behavior of the solution, is completely different from the mass spectrum. While nearly 90% of the mass is provided by molecules larger than 9 kD in MW, these MW fractions account for less than 30% of the total osmolality of the preparation, as the osmolality is based on the number of molecules. The "effective" osmolality of this solution is, however, based on the osmolality of each fraction times the corresponding lumped reflection coefficient in the three sets of membrane pores. In Figure 1B, this spectrum (% of total), that is, osmolality times the lumped σ for each fraction, is presented. Figure 1 underscores the importance of the larger size fractions as being more efficient osmolytes when compared with the smaller size fractions.

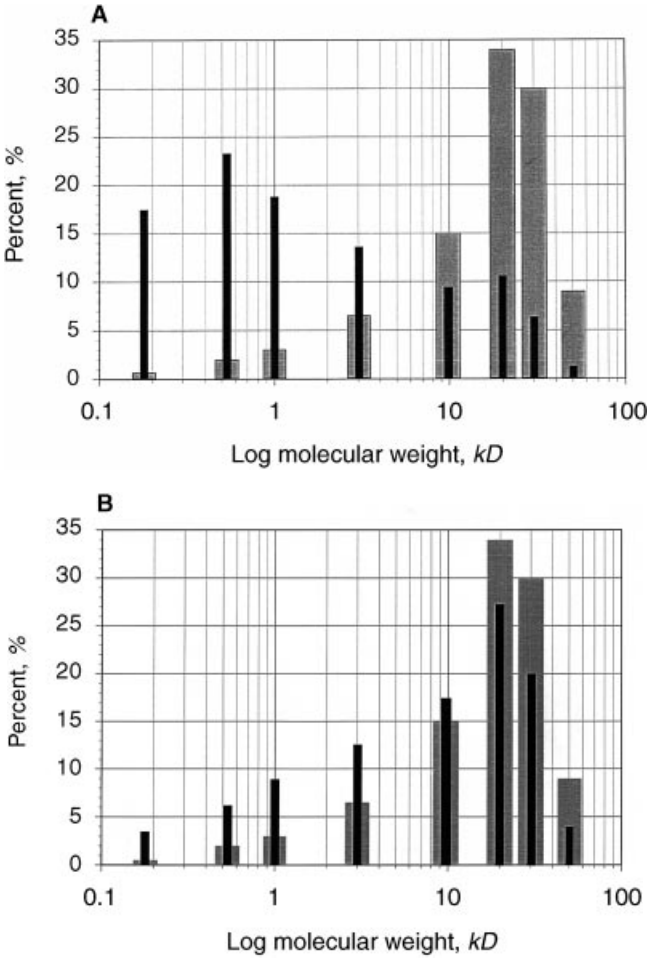

Fig. 1. (*A*) Mass and osmolality spectra of icodextrin. The osmolality spectrum (■), which critically determines the osmotic behavior of the solution, is completely different from the mass spectrum (▩). Whereas nearly 90% of the mass is provided by molecules larger than 9 kD in molecular weight (MW), these MW fractions represent less than 30% of the total osmolality of the dextrin preparation. (*B*) Mass spectrum and spectrum of "effective" osmolality of icodextrin. The "effective" osmolality spectrum (■), although prominent for the low MW fractions, largely follows the mass spectrum (▩).

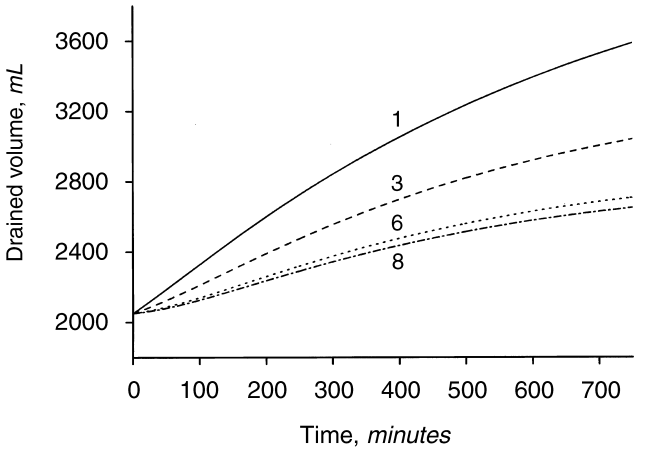

Fig. 2. Computer-simulated ultrafiltration (UF) profiles for 7.5% monodispersed 20 kD dextrin solution (denoted "1") in comparison with the icodextrin having the composition depicted in Figure 1, with eight major MW fractions (denoted "8"). Two preparations of intermediate "dispersion" are also shown. There is almost no difference between the UF profile simulated for six versus eight subfractions of the icodextrin preparations. The two lower curves seem to fit well with literature.

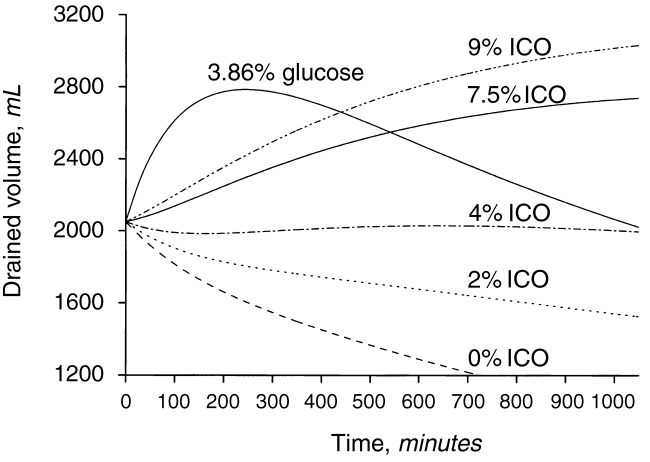

Fig. 3. Computer-simulated UF profiles for five different icodextrin concentrations (0 to 9% ICO) compared with that simulated for 3.86% glucose (G). The 4% ICO preparation seemed to be largely isovolumetric during 12 hours. After eight to nine hours, the UF volume for 7.5% icodextrin (polydispersed, 8 fractions) exceeded that for 3.86% glucose.

RESULTS

Impact of molecular size dispersion on the osmotic behavior of dextrin preparations

Figure 2 shows the simulated UF profiles for a 7.5% homogeneous 20 kD dextrin solution in comparison to an ICO solution with the composition depicted in Figure 1, having eight major MW fractions. Two preparations of intermediate dispersion are also shown. Note the small difference between the curves simulated using 6 versus 8 subfractions of the ICO preparation. The two lower curves seem to fit well the UF data reported in the literature for ICO [11–14]. Actually, the more dispersed solutions produced UF profiles similar to that simulated using only eight fractions (data not shown), that is, coinciding with the lower curve. In the next sections, computer simulations mainly based on the eight subfractions are presented.

Simulated UF profiles at various concentrations of ICO in previously unexposed patients

Figure 3 shows the computer-simulated UF profiles for five different ICO concentrations (0 to 9% ICO) compared with that simulated for 3.86% glucose [2]. Simulations were made using eight ICO subfractions (compare with Fig. 1), and the dwell time was extended to 17 hours (1020 min). A 7.5% ICO preparation seemed to yield a UF volume that was higher than that obtained

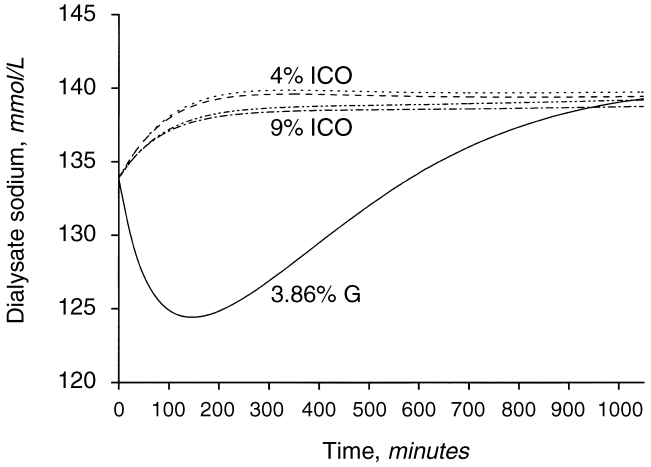

Fig. 4. Sodium sieving profiles for icodextrin (ICO) and 3.86% glucose (G). There is a near absence of sodium sieving for icodextrin (4% and 9%), whether given as a homogenous preparation (lower curve in each pair of curves), yielding a high degree of UF, or as a polydispersed solution (8 subfractions; upper curve in each pair denotes 4% ICO and 9% ICO). Sodium sieving for 3.86% glucose (G, lower solid line) is simulated for comparison.

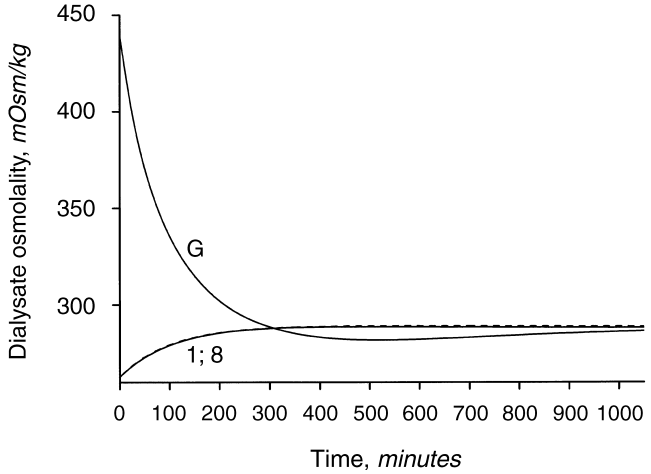

Fig. 5. Simulated dialysate osmolality versus dwell time for icodextrin (ICO, dashed line) and for 3.86% glucose (G, solid line) during a single dwell. Note that the ICO solution (whether homogeneous, "1", or polydispersed, "8") is simulated to be hypotonic during the first four to five hours of the dwell, in stark contrast to the situation for 3.86% G.

for 3.86% glucose after nine hours (≈500 mL). A 4% ICO preparation, however, seemed to be largely "isovolumetric" during 12 hours.

Sodium sieving profiles for ICO and for 3.86% glucose

Figure 4 demonstrates the near absence of sodium sieving for ICO whether given as a homogeneous preparation (lower curve in each pair of dextrin curves) for 4 and 9% ICO or as a polydispersed solution (8 subfractions; the upper curve in each pair). By contrast, the marked sodium sieving occurring for 3.86% glucose resulted from osmotic water flow through the aquaporins. Still, the fact that 9% ICO showed slightly lower dialysate sodium than 4% ICO indicates that the sodium sieving was not completely abolished even for ICO-based dialysis fluids.

Osmolality profiles for ICO and for 3.86% glucose during a single dwell

Figure 5 depicts dialysate osmolality as a function of dwell time for glucose and monodispersed (20 kD/fraction) ICO or polydispersed (8 fractions) ICO. The ICO solution was slightly hypotonic to plasma (plasma osmolality ≈290 mOsm/kg) during the first four to five hours of the dwell, in stark contrast to the situation for 3.86% glucose. This is due to the "colloidal" nature of ICO in comparison to any low MW osmotic agent.

Simulated UF profiles for 7.5% ICO in patients with steady-state plasma levels of ICO and its metabolites

In the present simulations, we preferred to show the UF profile data for patients previously unexposed to ICO.

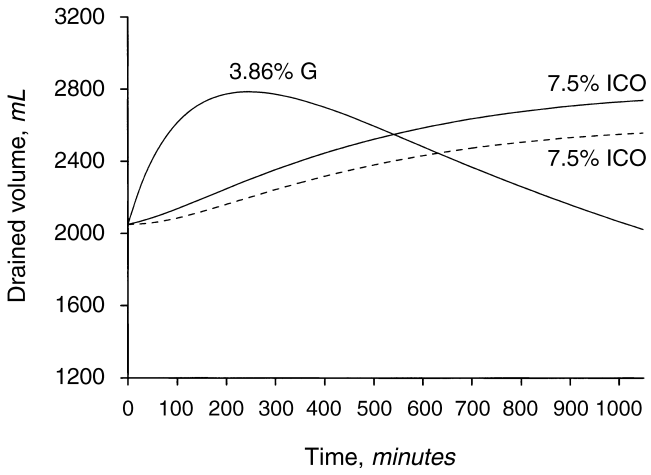

Fig. 6. Computed UF profiles for 7.5% icodextrin (ICO) in patients with long-term exposure to ICO (lower, dashed line curve) in comparison with patients exposed to 7.5% ICO for the first time. Simulations of plasma concentrations of ICO and ICO degradation products in the long-term patient were based on data from Davies and Posthuma et al [10, 17].

It should be noted, however, that patients with steady-state plasma levels of ICO and its metabolites following long-term ICO use showed significantly lower UF profiles than the previously unexposed patients, as illustrated in the simulation shown in Figure 6. For this simulation, published data were used and rearranged to fit the present model [10, 17]. Corresponding to the different size fractions, the following plasma ICO metabolite concentrations were used (the plasma glucose concentration is given in Table 1): 0.54 kD, 1.5 g/L; 1.0 kD, 1.3 g/L; 3.0 kD, 0.8 g/L; 10 kD, 0.6 g/L; and 20 kD, 0.4 g/L. Note that the UF volume in 17 hours was reduced from 670 to

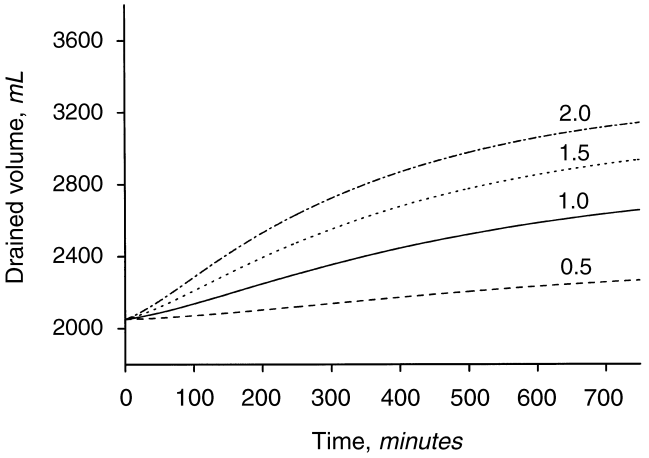

Fig. 7. Effects of alterations of the vascular surface area (area parameter, $A_0/\Delta X$) on UF profiles for 7.5% icodextrin. The surface area is varied from 50% of control (0.5) to twice the control value (2.0). Control curve is denoted by "1.0" (solid line). Note the marked increase in UF obtained when surface area is increased.

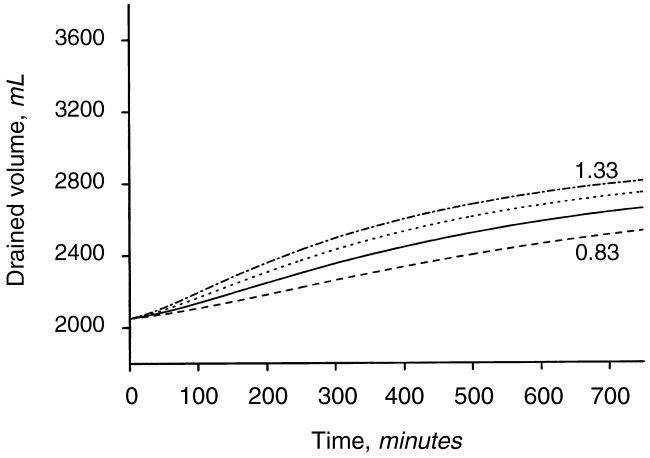

Fig. 8. A special condition of changes in vascular surface area, where for any step change in surface area (S), the permeablility-surface area [PS; mass transfer area coefficient (MTAC)] is altered in proportion to S, but the peritoneal UF-coefficient (L_pS) is only altered by one third (33%). The solid line symbolizes control situation (PS and LpS at control values). The dotted line depicts a situation in which PS is altered to 150% and LpS to 117% of control. Thus, if PS is doubled, L_pS is increased by 33% (denoted "1.33"), and when PS is reduced by 50%, L_pS is reduced to 83% of control value (denoted "0.83").

500 mL in the long-term patients. Furthermore, the UF volume at 12 hours in the long-term patients could be expected to be only 410 mL instead of 580 mL, and the time at which the UF volume for 7.5% ICO exceeded that of 3.86% glucose was 11 hours instead of 9 hours after long-term ICO treatment. In the following simulations, however, only the situation in patients who had not been previously exposed to dextrins is discussed.

Effects of alterations of vascular surface area on the UF profile of 7.5% ICO

Figure 7 demonstrates the computer-simulated change in UF profiles for 7.5% ICO that occurred when the (vascular) surface area ("area parameter"; $A_0/\Delta X$) varied from 50% of control (0.5) to twice the control value (2.0). Note the marked increase in UF obtained when the surface area was increased. By contrast, for 3.86% glucose, there was a reduction in UF after 200 minutes when the capillary surface area was increased (compare with Fig. 5 in [2]). This pattern of alterations is expected to occur in, for example, peritonitis, where ICO would be superior to glucose as an osmotic agent.

Effects of varying solute diffusion capacity more than the peritoneal UF coefficient

The scenario of simultaneous increases in PS and L_pS, where the increase in L_pS is less prominent than predicted from the changes in surface area (S) is common in so-called type-1 UF failure [18, 19]. Figure 8 depicts a condition in which for any step change in the surface area, PS (MTAC) was altered in proportion to S, but L_pS was only altered by one third. Thus, if PS was doubled, L_pS increased only by 33%. Again, although less pronounced than in Figure 6, ICO produced an improved UF profile compared with control when the (vascular) surface area was increased.

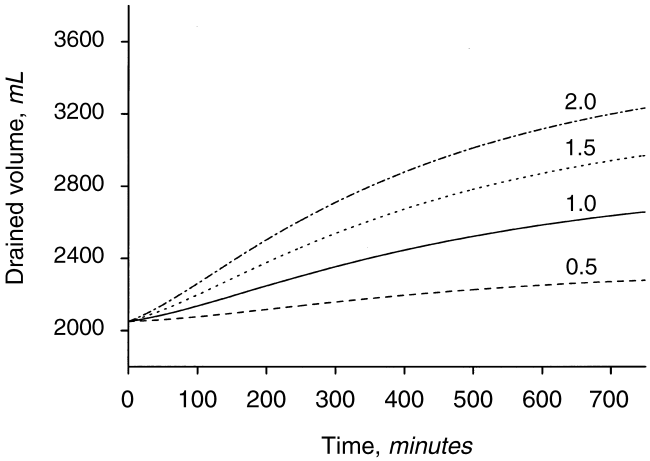

Fig. 9. Effects of varying the peritoneal UF coefficient (L_pS), but not the solute diffusion capacity (PS or MTAC) on UF profiles for 7.5% ICO. L_pS is varied from 50% of control ("0.5") to 100% above control ("2.0"), keeping the PS for small solutes constant. In this situation, there is a marked increase in UF transport with ICO. With G, the maximum UF volume after approximately 200 minutes is also increased with increasing L_pS.

Effects of varying the UF coefficient on the UF profiles for 7.5% ICO

When G was used as osmotic agent, increases in L_pS caused increases in both the initial UF and in reabsorption of fluid from the peritoneal cavity to plasma after four hours of the dwell [2]. The "height" of the UF

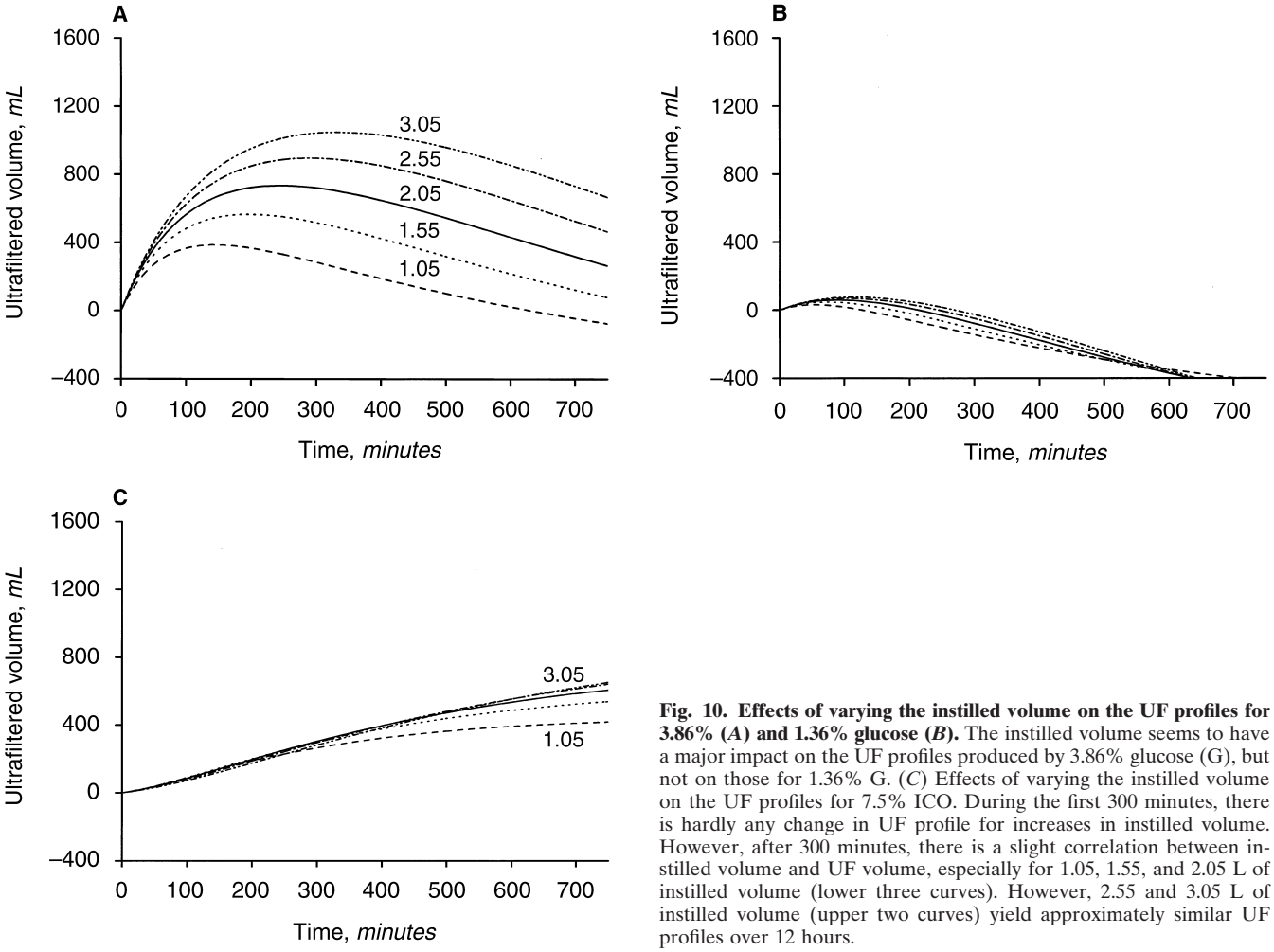

Fig. 10. Effects of varying the instilled volume on the UF profiles for 3.86% (*A*) and 1.36% glucose (*B*). The instilled volume seems to have a major impact on the UF profiles produced by 3.86% glucose (G), but not on those for 1.36% G. (*C*) Effects of varying the instilled volume on the UF profiles for 7.5% ICO. During the first 300 minutes, there is hardly any change in UF profile for increases in instilled volume. However, after 300 minutes, there is a slight correlation between instilled volume and UF volume, especially for 1.05, 1.55, and 2.05 L of instilled volume (lower three curves). However, 2.55 and 3.05 L of instilled volume (upper two curves) yield approximately similar UF profiles over 12 hours.

curve, but not the time to the curve peak (t_{peak}), increased markedly for increases in L_pS (compare with Fig. 6 in [2]). For ICO, there was also a marked, more or less proportional, increase in UF volume after 10 hours when L_pS was increased, as demonstrated in Figure 9, where L_pS varied from 0.5 of control to twice the control.

Effects of varying the instilled volume on the UF profiles for 7.5% ICO and for glucose

While the instilled volume apparently had a major impact on the UF profile produced by 3.86% glucose (Fig. 10A) [2], but not for 1.36% glucose (Fig. 10B), it only had a marginal effect on the UF profiles caused by 7.5% ICO (or 4% ICO; data not shown), as depicted in Figure 10C. In Figure 10, the instilled volume varied from 1.05 L (in 0.5 L steps) to 3.05 L and simulated versus UF volume. Note that 2.55 and 3.05 L of instilled ICO volumes yielded nearly identical UF profiles. A markedly increased UF volume is thus not to be expected from an increase in instilled ICO volume.

Effects of an increased direct lymphatic absorption on UF profiles for 7.5% ICO

When a high MW solute is placed in the peritoneal cavity, it will disappear by direct lymphatic absorption (L), by tissue absorption, and by varying degrees of capillary absorption. The direct peritoneal to plasma absorption of a large solute usually represents only a small fraction of the total disappearance of the solute. The tissue absorption of ICO in this study was set at 1.2 mL/min, which largely accounted for the discrepancy between total large solute clearance out of the peritoneal cavity and its "direct" lymphatic absorption (L) [20, 21]. Figure 11 shows how variations in direct lymphatic absorption affected the UF profile for 7.5% ICO. When L is 1.0, there was hardly any UF at all. For higher values of L, UF became negative. It has to be pointed out that, indeed, very high values of L are extremely uncommon clinically [21].

Effects of combining ICO with glucose

Figure 12A shows UF profiles for 7.5 and 4% ICO solutions, which also contained 1.36% glucose. An ICO

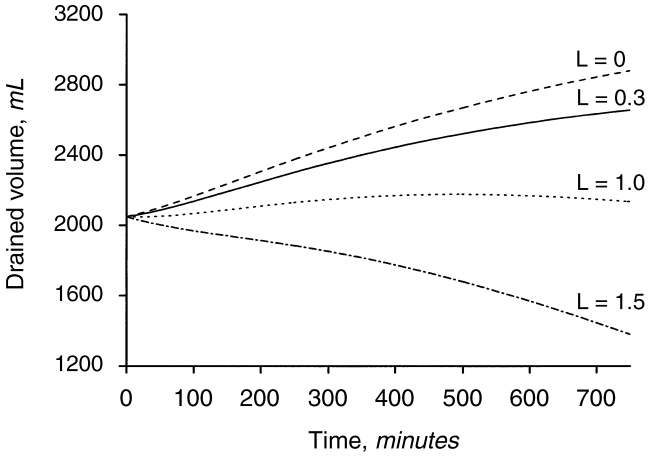

Fig. 11. Drained volume versus time curves for 7.5% ICO obtained at variations of the direct lymphatic absorption (L). The UF profile is largely "isovolumetric" for L = 1.0 (mL/min), but becomes negative for higher values of direct lymphatic absorption.

of 7.5% and 4% are shown for comparison. Glucose actually produced a marked initial UF and ICO maintained this UF level during the 12-hour dwell. Even a 4% ICO solution yielded a favorable UF volume at 10 to 12 hours. Figure 12B shows the dialysate Na as a function of dwell time for the curves shown in Figure 12A. Because of the presence of rather high concentrations of a low MW osmotic agent (glucose), the Dex/glucose solutions caused significant sodium sieving, unlike the pure Dex solutions, which produced weak, or absent, reductions in dialysate sodium.

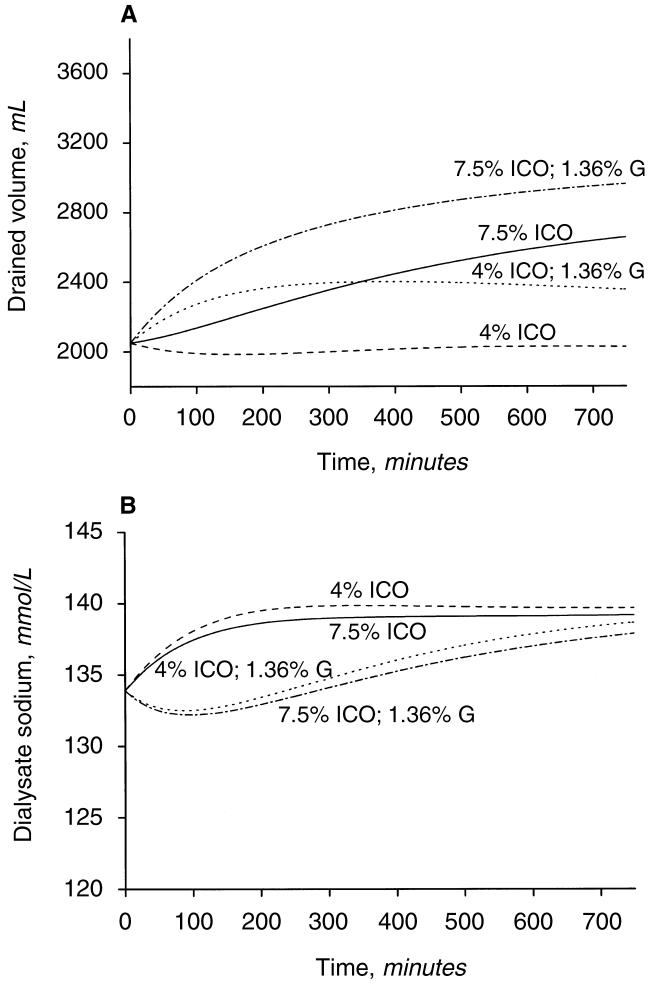

Fig. 12. (*A*) Simulated UF profiles for combinations of 1.36% G with 4% (dotted line) or 7.5% (solid line) ICO solutions. Note that the presence of low MW osmotic agents (G) initially yields a significant UF. The presence of ICO will maintain the UF rate more or less constant following the first 300 minutes of the dwells. (*B*) Sodium sieving curves corresponding to the curves in Figure 10A. Note that only the G containing dialysis fluid causes significant sodium sieving.

DISCUSSION

To correctly computer simulate the osmotic behavior of ICO, it is necessary to consider its polydispersed nature. Actually, the difference in osmotic behavior between a homogenous dextrin having a MW of 20 kD and a polydispersed dextrin with a weight average MW of 20 kD and a number average MW of approximately 6 kD [10] is very pronounced. Taking into consideration the polydispersity of ICO, it could be shown, however, that it is sufficient to subdivide the dextrin molecules into six to eight different MW (or size) fractions. Further subdividing the osmotic molecules into more fractions did not produce any further changes in UF profiles compared with that generated with only eight fractions. In the present simulations, however, we did not take into account any degradation of high MW dextrins into low MW dextrins, as proposed from rat experiments [22]. It should be pointed out that even when completely undegraded, the majority of osmotically active dextrin molecules (≈70%) are in the low MW range (<3 kD), despite the fact that most of the molecular mass (80%) is provided by molecules in the high-MW mass range. Still, since the solute osmotic efficiency will increase with increases in molecular size, the UF contribution of the different molecular size fractions, although more pronounced for the low MW solutes, will be largely in proportion to the molecular mass spectrum.

According to the present simulations and in agreement with the study by Ho-dac-Pannekeet et al in humans [14], ICO remained hypotonic compared with plasma during the first two hours of the dwell. Furthermore, the rate of net UF was initially quite low, but increased slightly over the first to second hours of the dwell in order to remain steadily increased for up to 10 hours of the dwell. Indeed, the UF volume did not reach a maximum during the first 12 hours after fluid instillation. The reason for the initial slight depression of UF rate was the initial crystalloid osmotic imbalance between plasma

and dialysate, particularly concerning the concentrations of urea and glucose, which were initially near zero in the dialysate but high in plasma (especially for urea). This is evident from computer simulations in which glucose, sodium, and urea concentration gradients across the peritoneum were set at zero (data not shown). Normally, these crystalloid (small solute) osmotic pressures gradually dissipate over the first two to three hours of the dwell, particularly when urea has equilibrated across the peritoneum. In animal studies, the contribution of initial degradation of large MW dextrins into low MW dextrins and the fact that the osmolytes have to diffuse to the capillary walls to exert their effect (discussed later in this article) may also contribute to an increasing osmotic capacity of the dialysis fluid developing with increasing dwell time [22].

Overall, the general UF behavior of the simulated 7.5% ICO solution is in accordance with previously published data. In the MIDAS study, the long-term patients (5 months) produced a UF volume of 510 ± 260 (± SD) mL at 8 hours and of 550 ± 240 mL at 12 hours [11–13]. Previously unexposed patients, in accordance with the present simulations, produced a higher UF volume: 710 ± 350 mL in eight hours. In the present simulations, 7.5% ICO produced the same cumulative amount of net UF as 3.86% glucose at nine hours in previously unexposed patients. In patients showing steady-state plasma levels of ICO and its metabolites, this occurred at ~11 hours. The present simulations are also in rough agreement with measured and extrapolated values from more detailed dwell studies in humans [14], where the degree of sodium sieving was also studied. In agreement with the present results, the dialysate to plasma concentration ratio (D/P) for sodium remained more or less a constant over time during the first few hours of the dwell; that is, no significant sodium sieving was observed with ICO [14]. In another recent study of automatic PD (APD) patients [23], "daytime" UF volume with 7.5% ICO during 12 months of follow-up was only 204 ± 95 mL (± SEM), which is lower than simulated in our study and much lower than indicated from the MIDAS study or the dwell study of Ho-dac-Pannekeet et al [14]. The reason for this discrepancy is not known. Generally, however, there is a lack of data on the UF properties of ICO during long dwells, and it is speculated that the data of Posthuma et al may be representative of a cohort of patients showing relatively low values of the peritoneal UF coefficient (L_PS; discussed later in this article) [17].

Ultrafiltration failure (UFF) is a frequent complication of long-term CAPD. In six years, the risk of developing UFF is approximately 30% [18]. The most frequent cause of UFF is probably an increased effective vascular surface area (increased $A_0/\Delta X$) [18, 19]. The present simulations clearly show an advantage of using ICO in patients with this condition [25]. Thus, in contrast to the situation when glucose is used as an osmotic agent, ICO will actually produce an enhanced UF rate when the vascular surface area is increased. A doubling of the effective vascular surface area implies a near doubling of the UF volume with ICO (from ~580 to 1100 mL) at 12 hours in patients who were not previously exposed to ICO. This increase in UF occurs under the provision that both L_pS and PS will increase as a result of the enhanced vascular surface area. To the extent that L_pS is increased less than the increase in PS, when vascular surface area is increased, the improvement in UF profile with ICO will be less pronounced [26]. Anyway, it can be predicted that most UFF patients will actually improve their UF during ICO dwells compared with non-UFF patients. It should be noted, however, that in the rare cases when the UFF depends on a high "direct" lymphatic absorption rate (L), there would hardly be an advantage of using ICO, as demonstrated in the present simulations.

For patients classified as "high" or "high average" transporters according to the peritoneal equilibration test (PET) [27], a similar reasoning as for the UFF patient applies. It is probable that a high or high average transporter has a higher effective vascular surface area than the "low" or "low average" transporter. Again, to the extent that the vascular surface area, and hence L_pS, is increased in the high average transporters [26], they will show an improved UF response as compared with low or low average transporters.

Whereas the instilled volume was of great importance in determining the UF profiles for hypertonic glucose [2, 24], the impact of the instilled volume on UF with 7.5% ICO was rather marginal. Actually, during the first five hours of the dwell, the UF profiles looked almost exactly the same whether the instilled volume was 1.05 or 3.05 L. However, between 5 and 12 hours, there was some separation of the curves, implying some improvement of UF volume for the higher instilled volumes. However, all in all, there is no major rationale for increasing the instilled volume to improve UF with ICO. The negligible impact of instilled volume on UF volume for 1.36% glucose is a bit surprising, but fits very well with recent data in rats [24]. Indeed, in that animal study, increases in instilled volume produced improved UF for 3.86% glucose in accordance with previous simulations [2]. However, for 1.36% glucose, increases in instilled volume tended to impair the UF capacity. In the present simulations, such an impairment seemed to occur after 500 minutes of dwell time. This phenomenon would have been even more marked, however, if intraperitoneal hydrostatic pressure (IPP) had been simulated to increase in a more exaggerated fashion as a function of intraperitoneal volume (compare with Eq. 2, **Appendix**) than in the present study. The slight discrepancy between the computer simulations and the above-mentioned UF data in rats can thus be readily explained.

Combining low concentrations of glucose (for example, 1.36% glucose) with 7.5% ICO will produce a marked initial UF, usually followed by a steady UF rate over time, resulting in more than 800 mL of UF volume in 12 hours for the mentioned ICO/glucose formulation. Also, 4% dextrin together with 1.36% glucose will result in approximately 300 mL of UF volume in 10 to 12 hours. In a recent study in rats, the addition of low concentrations of glucose to ICO did not seem to markedly improve UF in a four-hour dwell, but did improve it in two hours [24]. It should be noted, however, that the fluid kinetics in a rat is markedly different from that in humans in that the UF profiles are "compressed" in time by a factor of 2 to 3 in rats. Furthermore, in the mentioned rat study, there were indications of degradation of high MW dextrins into low MW dextrins, which were not considered in the present simulations. This may account for the observed differences.

The general validity and applicability of the three-pore model of peritoneal transport has been discussed at some length elsewhere [1, 2, 8, 9, 15], but some additional aspects with particular relevance to the situation of employing macromolecules as osmotic agents should be considered here. In particular, in the mentioned study of rats, there was an initial delay in UF after the instillation of the ICO containing dialysis fluid [24]. Part of this initially reduced UF is obviously due to the presence of initial crystalloid osmotic imbalances between in plasma and dialysate, as discussed previously in our article. Part of the delay may also be due to the fact that the capillary membrane (endothelium) is not in direct contact with the dialysate, but instead is distributed within the matrix of the interstitium. In such a distributed model [28, 29], there may be a significant interstitial diffusion resistance to large solutes, producing a delay in the establishment of a full osmotic force across the endothelium. Furthermore, in a distributed model of peritoneal transport, any changes in the anatomical endothelial surface area will not produce directly proportionate changes in overall solute transport. For example, a doubling of the endothelial surface area would theoretically result in only an approximately 45% increase of overall transperitoneal diffusion capacity [28]. In the present study, such effects were not accounted for, and the term "surface area" was used in the sense of it being "effective" vascular surface area. Despite the fact that the three-pore model does not account for the impact of the interstitial matrix on transport, it is intriguing to note that the predictions obtained using a simple "membrane model" seem to be in good agreement with the reported data, as discussed previously in this article. The error of not taking into account the impact of transport resistances in the interstitium may thus, after all, be rather minor.

In summary, the polydispersed nature of ICO has to be taken into account in computer simulations of UF profiles induced by ICO dwells. In long-term patients, the accumulation of ICO and ICO metabolites in plasma also significantly impacts on the simulated UF profiles. By applying the three-pore model of peritoneal transport, we obtained UF profiles that were remarkably similar to those reported in the literature. Furthermore, it was possible to make a number of generalizations based on the simulations. The major implication of our simulations is that UFF, when caused by increases in both small solute permeability-surface area (MTAC) and membrane UF coefficient, has a clearly positive influence on UF rate and UF volumes when 7.5% ICO is used as the osmotic agent. However, changes in instilled fluid volume will only marginally affect the UF profile when ICO is used as osmotic agent in peritoneal dialysis.

ACKNOWLEDGMENTS

This study was supported by grants from the Swedish Medical Research Council no. 08285, the Zoega Foundation, and Lundberg Foundation. We are very grateful to Dr. Martin Wilkie, Northern General Hospital, Sheffield, UK, for valuable suggestions and discussions in the early phase of this study. Ms. Kerstin Wihlborg is gratefully acknowledged for her skill in typing the manuscript. Part of this study was published as an abstract (*J Am Soc Nephrol* 9:301A, 1998).

Reprint requests to Dr. Bengt Rippe, Department of Nephrology, University of Lund, S-221 85 Lund, Sweden.

APPENDIX

According to the three-pore model [1, 2], the changes in peritoneal volume (V_D) with time can be described by the following:

$$\frac{dV_D}{dt} = J_{V_C} + J_{V_S} + J_{V_L} - L \qquad \text{(Eq. 1)}$$

where J_{V_C}, J_{V_S}, and J_{V_L} represent the fluid flows through transcellular, small pores, and large pores, respectively, and L stands for the peritoneal lymph flow, which is fixed here to 0.3 mL/min. Each of the fluid flows is given by [2]:

$$J_{V_{pore}} = \alpha_{pore} L_p S[\Delta P(V_D) - \sum_{solute} \sigma_{pore,solute} \Delta\pi_{solute}(t)] \qquad \text{(Eq. 2)}$$

where α_{pore} stands for the "fraction of L_pS" accounted for by the specific set of pore; L_pS is the membrane UF-coefficient; and ΔP represents the hydrostatic pressure difference between the blood capillaries and the peritoneal cavity, which is calculated according to [30]:

$$\Delta P(V_D) = \Delta P(2050 + V_r) - \frac{V_D(t) - (2050 + V_r)}{490} \qquad \text{(Eq. 3)}$$

where V_r is the peritoneal residual volume (300 mL). In equation 2, the sum is taken for all of the solutes. The solutes used in this study are glucose, urea, eight fractions of Icodextrin, plasma proteins, sodium (Na^+), and its anions. The last two crystalloid osmotic transients were treated numerically as twice the sodium osmotic transient multiplied by a dissociation factor (0.93). The symbol σ represents the osmotic reflection coefficient, calculated by [31]:

$$\sigma_{pore,solute} = 1 - \frac{(1 - \lambda)^2[2 - (1 - \lambda)^2](1 - \lambda/3)}{1 - \lambda/3 + 2/3\lambda^2} \qquad \text{(Eq. 4)}$$

where λ is the solute radius (α_e) over pore radius (r_{pore}). According to van't Hoff's law, the ideal crystalloid osmotic gradients (in mm Hg), Δ, acting across the peritoneal membrane, are calculated from:

$$\Delta\pi_{solute}(t) = RT[C_{P,solute} - C_{D,solute}(t)] \qquad \text{(Eq. 5)}$$

where RT (the product of the gas constant and the temperatures in degrees Kelvin) is 19.3 mm Hg/mmol/L; C_P is the plasma solute concentration; and $C_D(t)$ is the concentration of solute in the dialysate as a function of dwell time. For plasma proteins, the $\Delta\pi$ was set constant at 22 mm Hg during the dwell. The changes of the mass (m) of a solute versus time (mmol/min) in the peritoneal cavity can be described by:

$$\frac{dm_{solute}}{dt} = J_{S_{S,solute}} + J_{S_{L,solute}} - \frac{LC_{D,solute}(t)}{1000} \quad \text{(Eq. 7)}$$

where L is the peritoneal lymph flow; $C_D(t)$ is the dialysate concentration of solute; $J_{S_{S,solute}}$ is the solute flux through small pores and $J_{S_{L,solute}}$ through the large pores. A "1000" in the denominator of the third term to the right is a conversion factor for L (from mL/min to L/min). Each of the solute fluxes is given by:

$$J_{S_{pore,solute}} = \frac{J_{V_{pore}}(1 - \sigma_{pore,solute})}{1000} \frac{(C_{P,solute} - C_{D,solute}(t) \cdot e^{-Pe_{pore,solute}})}{(1 - e^{-Pe_{pore,solute}})} \quad \text{(Eq. 8)}$$

Pe in Equation 8 is a modified Peclet number, defined by:

$$Pe_{solute,pore} = J_{V_{pore}} \frac{(1 - \sigma_{pore,solute})}{PS_{solute,pore}} \quad \text{(Eq. 9)}$$

where the permeability surface area (PS; mL/min), unless otherwise stated in Table 1, is defined by:

$$PS_{solute,pore} = D_{solute}\left(\frac{A_0}{\Delta x}\right)_{pore}\left(\frac{A}{A_0}\right)_{solute,pore} \cdot 60 \quad \text{(Eq. 10)}$$

Here $A_0/\Delta X$ is the "unrestricted" pore area over diffusion path length, and D_{solute} represents the free solute diffusion coefficient (in cm^2/s). A/A_0 in equation 10 represents a factor determining the degree of restricted to free diffusion occurring across the permeable pathways under study. According to pore theory, A/A_0 is a function of solute radius over pore radius, denoted λ. We have employed the following relationship to describe this parameter [31]:

$$\left(\frac{A}{A_0}\right)_{solute,pore} = \frac{(1 - \lambda)^{4.5}}{1 - 0.3956\lambda + 1.0616\lambda^2} \quad \text{(Eq. 11)}$$

For transport in the peritoneal-to-plasma direction, 1.2 mL/min (to account for tissue absorption of dextrins) was added to the otherwise calculated PS values. The PS for glucose, Na and anions were, however, set prefixed according to Table 1 (provided that surface area "S" was kept unchanged). The alterations in $C_D(t)$ with time were obtained from simple mass considerations:

$$\frac{dm_{solute}}{dt} = \frac{d(C_{D,solute}V_D)}{dt} = \frac{dC_{D,solute}}{dt}V_D + C_{D,solute}\frac{dV_D}{dt} \quad \text{(Eq. 12)}$$

from with we can extract the relationship:

$$\frac{dC_{D,solute}}{dt} = \frac{1}{V_D}\left[\frac{dm_{solute}}{dt} - C_{D,solute}\frac{dV_{D,solute}}{dt}\right] \quad \text{(Eq. 13)}$$

The sets of equations that need to be integrated numerically are the volume versus time function and all of the solute concentrations versus time. In order to calculate the initial concentrations, the following equation was used:

$$C_{D,solute}(0) = \frac{V_I C_{I,solute} + V_r C_{r,solute}}{V_I + V_r} \quad \text{(Eq. 15)}$$

where V_I is the volume of the dialysis fluid, prior to instillation, C_I the dialysis fluid solute concentration in the bag, V_r the residual volume, and C_r is the solute concentration in the residual volume. This was set equal to the plasma concentration. The initial volume was:

$$V_D = V_I + V_r \quad \text{(Eq. 16)}$$

REFERENCES

1. Rippe B, Stelin G: Simulations of peritoneal solute transport during CAPD: Application of two-pore formalism. *Kidney Int* 35:1234–1244, 1989
2. Rippe B, Stelin G, Haraldsson B: Computer simulations of peritoneal fluid transport in CAPD. *Kidney Int* 40:315–325, 1991
3. Agre P, Preston BM, Smith BL, Jung JS, Raina S, Moon C, Guggino WB, Nielsen S: Aquaporin CHIP: The archetypal molecular water channel. *Am J Physiol* 265:F463–F476, 1993
4. Carlsson O, Nielsen S, Zakaria ER, Rippe B: *In vivo* inhibition of transcellular water channels (aquaporin-1) during acute peritoneal dialysis in rats. *Am J Physiol* 271:H2254–H2262, 1996
5. Pyle WK, Moncrief JW, Popovich RP: *Peritoneal Transport Evaluation in CAPD: CAPD Update, Continuous Ambulatory Peritoneal Dialysis. New York, Mason Publishing*, 1981, pp 35–42
6. Vonesh EF, Lysaght MJ, Moran J, Farrell P: Kinetic modelling as a prescription aid in peritoneal dialysis. *Blood Purif* 9:246–270, 1991
7. Rippe B, Zakaria ER, Carlsson O: Theoretical analysis of osmotic agents in peritoneal dialysis. What size is an ideal osmotic agent? *Perit Dial Int* 16(Suppl 1):S97–S103, 1996
8. Rippe B: A three-pore model of peritoneal transport. *Perit Dial Int* 13(Suppl 1):S35–S38, 1993
9. Vonesh EF, Rippe B: Net fluid absorption under membrane transport models of peritoneal dialysis. *Blood Purif* 10:209–226, 1992
10. Davies DS: Kinetics of icodextrin. *Perit Dial Int* 14(Suppl 2):S45–S50, 1994
11. Mistry CD, Gokal R: Icodextrin in peritoneal dialysis: Early development and clinical use. *Perit Dial Int* 14(Suppl 2):S13–S21, 1994
12. Gokal R, Mistry CD, Peers E, MIDAS Study Group: A United Kingdom multicenter study of icodextrin in continuous ambulatory peritoneal dialysis. *Perit Dial Int* 14(Suppl 2):S22–S27, 1994
13. Mistry CD, Gokal R, Peers EM, MIDAS Study Group: A randomized multicenter clinical trial comparing isoosmolar icodextrin with hyperosmolar glucose solutions in CAPD. *Kidney Int* 46:496–503, 1994
14. Ho-dac-Pannekeet MM, Schouten N, Langendijk MJ, Hiralall JK, de Waart DR, Struijk DG, Krediet RT: Peritoneal transport characteristics with glucose polymer based dialysate. *Kidney Int* 50:979–986, 1996
15. Stelin G, Rippe B: A phenomenological interpretation of the variation in dialysate, with dwell time in CAPD. *Kidney Int* 38:465–472, 1990
16. Haraldsson B: Assessing the peritoneal dialysis capacities of individual patients. *Kidney Int* 47:1187–1198, 1995
17. Posthuma N, Wee M, Donker JM, Oe L, van Dorp W, Peers E, Verburgh H: Serum disaccharides and osmolality in CCPD patients using Icodextrin or glucose as daytime dwell. *Perit Dial Int* 17:602–607, 1997
18. Heimbürger O, Waniewski J, Werynski A, Tranaeus A, Lindholm B: Peritoneal transport in CAPD patients with permanent loss of ultrafiltration capacity. *Kidney Int* 38:495–505, 1990
19. Rippe B: How to measure ultrafiltration failure: 2.27% or 3.86% glucose? (editorial) *Perit Dial Int* 17:125–128, 1997
20. Rippe B, Stelin G, Ahlmén J: Lymph flow from the peritoneal cavity in CAPD patients, in *Frontiers in Peritoneal Dialysis, 4*, edited by Maher JF, Winchester JF, New York, Field, Rich and Ass, Inc., 1986, pp 24–30
21. Heimbürger O, Waniewski J, Werynski A, Sun Park M, Lindholm B: Lymphatic absorption in CAPD patients with loss of ultrafiltration capacity. *Blood Purif* 13:327–339, 1995
22. Wang T, Heimbürger O, Cheng HH, Bergström J, Lindholm B: Peritoneal fluid and solute transport with different polyglucose formulations. *Perit Dial Int* 18:193–203, 1998
23. Posthuma N, Wee PM, Verburgh HA, Oe PL, Peers E, Sayers J, Donker AJM: Icodextrin instead of glucose during the daytime dwell in CCPD increases ultrafiltration and 24-h dialysate creatinine clearance. *Nephrol Dial Transplant* 12:550–553, 1997
24. Wang T, Heimbürger O, Cheng H, Waniewski J, Bergström J, Lindholm B: Effects of dialysate fill, on peritoneal fluid and solute transport. *Kidney Int* 52:1068–1076, 1997

25. Douma CE, Hiralall JK, de Waart DR, Struijk DG, Krediet RT: Icodextrin with nitroprusside increases ultrafiltration and peritoneal transport during long CAPD dwells. *Kidney Int* 53:1014–1021, 1998
26. Waniewski J, Heimbürger O, Werynski A, Lindholm B: Osmotic conductance of the peritoneum in CAPD patients with permanent loss of ultrafiltration capacity. *Perit Dial Int* 16:488–496, 1996
27. Twardowski ZJ, Nolph KD, Khanna R: Peritoneal equilibration test. *Perit Dial Bull* 7:138–148, 1987
28. Dedrick RL, Flessner MF, Collings JM, Schultz JS: Is the peritoneum a membrane? *ASAIO J* 5:1–8, 1982
29. Flessner MF: Peritoneal transport physiology: Insights from basic research. *J Am Soc Nephrol* 2:122–135, 1991
30. Twardowski ZJ, Prowant BF, Nolph KD, Martinez AJ, Lampton LM: High, low frequency continuous ambulatory peritoneal dialysis. *Kidney Int* 23:64–70, 1983
31. Mason EA, Wendt RP, Bressler EH: Similarity relations (dimensional analysis) for membrane transport. *J Membr Sci* 6:283–298, 1980